Journal of Power Sources 242 (2013) 884–894

Contents lists available at SciVerse ScienceDirect

Journal of Power Sources

journal homepage: www.elsevier.com/locate/jpowsour

Configuring a fuel cell based residential combined heat and power system☆

Shabbir Ahmed, Dionissios D. Papadias*, Rajesh K. Ahluwalia

Argonne National Laboratory, 9700 S. Cass Avenue, Lemont, IL 60439, USA

HIGHLIGHTS

- The distribution between heat and electrical efficiency of a CHP system has been analyzed.
- Design trade-offs are based on system start-up, electrical efficiency and heat output.
- These systems can operate at electrical and total efficiencies of ~46% and ~90%

ARTICLE INFO

Article history:
Received 27 September 2012
Received in revised form
3 January 2013
Accepted 5 January 2013
Available online 12 January 2013

Keywords:
Fuel cell
Polymer electrolyte
Heat and power
CHP
Systems analysis

ABSTRACT

The design and performance of a fuel cell based residential combined heat and power (CHP) system operating on natural gas has been analyzed. The natural gas is first converted to a hydrogen-rich reformate in a steam reformer based fuel processor, and the hydrogen is then electrochemically oxidized in a low temperature polymer electrolyte fuel cell to generate electric power. The heat generated in the fuel cell and the available heat in the exhaust gas is recovered to meet residential needs for hot water and space heating. Two fuel processor configurations have been studied. One of the configurations was explored to quantify the effects of design and operating parameters, which include pressure, temperature, and steam-to-carbon ratio in the fuel processor, and fuel utilization in the fuel cell. The second configuration applied the lessons from the study of the first configuration to increase the CHP efficiency. Results from the two configurations allow a quantitative comparison of the design alternatives. The analyses showed that these systems can operate at electrical efficiencies of ~46% and combined heat and power efficiencies of ~90%.

1. Introduction

Small combined heat and power (CHP) systems, which are a boon for remote locations, are also very attractive for residential power generators (DG) even for urban locations. These systems are capable of extracting a high percentage of the energy from the fuel in the form of electric power and heat (for space heating and/or hot water). Deployed in significant numbers, this network of distributed generators can mitigate the peak demand on the grid [1]. These systems can be integrated with the grid using strategies that balance the needs and risks of both the DG and the grid. The CHP systems can be deployed at various scales, ranging from residential (1–10 kWe) to large buildings, industry and even communities [2–4].

The owner of the CHP system benefits from the combination of higher fuel conversion efficiency – translating to lower cost of fuel per unit of energy, the availability of high quality power, the ability to rapidly vary the distribution between electric and thermal loads [5], and potential credit for any power contributed back to the grid. In cases of natural disasters such as tornadoes, hurricanes, tsunamis, etc., these units can continue to operate if the natural gas supply is not interrupted [6,7].

Polymer electrolyte fuel cell based systems are being developed for the residential application [5,8–14], fueled by available infrastructure fuels that include natural gas, liquefied petroleum gas, or petroleum derived fuels such as kerosene [11,15–18]. The heat generated by the stack, at 60–80 °C for the low temperature PEFC (LTPEFC) and ~150 °C for the high temperature PEFC (HTPEFC), is at a sufficiently high temperature to provide space heating and hot water for residential use [19]. Although the initial capital cost remains high (~$35,000 in Japan [20]), the estimated operating cost of electricity generation is competitive, at less than 10 cents/kW h assuming $1.20 per therm (35 kW h) of natural gas [21]. With large

☆ *The U.S. Government retains for itself, and others acting on its behalf, a paid-up, nonexclusive*irrevocable worldwide license in said article to reproduce, prepare derivative works, distribute copies to the public and perform publicly and display publicly, by or on behalf of the Government.

* Corresponding author. Tel.: +1 630 252 3206.
E-mail addresses: papadias@anl.gov, dennis.papadias@gmail.com (D.D. Papadias).

0378-7753/$ – see front matter © 2013 Elsevier B.V. All rights reserved.
http://dx.doi.org/10.1016/j.jpowsour.2013.01.034

Abbreviations and acronyms

C1, C2	System Configurations
CHP	Combined Heat and Power
DC	Direct Current
DOE	U.S. Department of Energy
FC	Fuel Cell
FP	Fuel Processor
HTPEFC	High Temperature Polymer Electrolyte Fuel Cell
HTS (WGS1)	High Temperature Water Gas Shift Reactor
kWe	Kilowatt Electric
LHV	Lower Heating Value
LTPEFC	Low Temperature Polymer Electrolyte Fuel Cell
LTS (WGS2)	Low Temperature Water Gas Shift Reactor
PEFC	Polymer Electrolyte Fuel Cell
ppm	Parts per Million
PrOx	Preferential Oxidation Reactor
SSH	Steam Superheater
S/C	Steam-to-Carbon Molar Ratio
SR	Steam Reformer
WGS1, WGS2	High and Low Temperature Water Gas Shift Reactor
η	Efficiency

Subscripts

CHP	Combined Heat and Power
El	Electric
EE	Electric Energy
FP	Fuel Processor

scale manufacturing (50,000 units per year), the cost of the fuel cell based CHP units are expected to range from \$7500 kWe^{-1} for 1 kWe units to \$2450 kWe^{-1} for 5 kWe LTPEFC based units [22].

Higher temperature fuel cells with their higher temperature (i.e., higher quality) waste heat are expected to yield higher CHP efficiencies [19]. CHP systems based on other types of fuel cells, such as phosphoric acid, molten carbonate, or solid oxide fuel cells have not been reported in commercial development for the residential application. Considerations weighing against the higher temperature fuel cells include the longer start-up time and the fuel penalty associated with the higher thermal mass (mass × heat capacity × difference between ambient and operating temperature).

This study has been limited to the analysis of only the LTPEFC CHP systems. The objective of this study has been to gain an understanding of these systems – the performance parameters and their sensitivity to design and operating parameters, and the tradeoffs that are possible.

2. The fuel cell system

The infrastructure fuel (natural gas in this case, which for simplicity is assumed to be 100% methane) is first converted to a hydrogen-rich gas suitable for the electrochemical oxidation in the fuel cell. Following this train of operations, this paper begins the analysis of the fuel cell based CHP systems with the fuel processor. The objective of this work was to establish the effect of the fuel processor (FP) layout, and the design and operating parameters on performance parameters such as hydrogen yields from the FP, power and heat outputs, and efficiencies of the FP and the overall CHP system. Future studies will incorporate these findings and incorporate them into studies exploring the effect of the fuel cell stack design and operating parameters.

Fig. 1 shows a generic schematic of a CHP system showing the principal subsystems: the fuel processor, the fuel cell stack, the power conditioner, and a coolant system that transfers heat within the system and to the external heat sink (residential heating needs). The arrows indicate possible feed and energy inputs and outputs. The fuel processor converts the primary fuel (methane) into a hydrogen-rich gas (>75% H_2, balance CO_2, with small amounts of CO, N_2, and other species) that is fed to the fuel cell anode. The hydrogen in the reformate is electrochemically oxidized with air in the fuel cell stack to generate direct current (DC) electric power. The unreacted hydrogen in the anode exhaust, along with the other species in the reformate, is fed to a burner, where it is combusted with air to generate heat. This heat is used to provide the heat of reaction for the endothermic reforming reaction; in some cases, supplemental methane may also be fed to the burner, such as during start-up or when the energy contained in the anode effluent is insufficient to meet all of the reformer demand.

The electrochemical reaction in the fuel cell generates electric power and heat. The latter is taken up by a coolant system and used to meet the application demands (space heating, hot water). Heat is also recovered from the post-reforming reactors in the fuel processor, a large fraction of which is used for preheating the reformer feeds, while some may be recovered and used for the external heat load.

The efficiencies for the system are defined by Eqs. (1)–(3).

$$\eta_{FP} = \frac{(\mathrm{LHV}_{H_2} \text{ to Fuel Cell})}{(\mathrm{LHV}_{Fuel}) + (\mathrm{LHV}_{H_2} \text{ in Anode Effluent}) + (\text{Heat}) + \dfrac{\text{Electric Energy}}{\eta_{EE}}} \times 100 \quad (1)$$

$$\eta_{El} = \frac{\text{Net Electric Energy Produced by Fuel Cell}}{(\mathrm{LHV}_{Fuel}) + (\text{Heat}) + \dfrac{\text{Electric Energy}}{\eta_{Grid}}} \times 100 \quad (2)$$

$$\eta_{CHP} = \frac{(\text{Net Electric Energy Produced by Fuel Cell}) + (\text{Heat})}{(\mathrm{LHV}_{Fuel}) + (\text{Heat}) + \dfrac{\text{Electric Energy}}{\eta_{Grid}}} \times 100 \quad (3)$$

Eq. (1) defines the efficiency of the fuel processor as the lower heating value of the hydrogen in the reformate product from the fuel processor, as a percentage of the sum of the LHV of the fuel (methane) feed into the FP, the LHV of the hydrogen in the fuel cell anode exhaust that is fed to the FP burner, any heat inputs from the fuel cell or external sources (e.g., steam from a nearby power plant, etc.) into the FP, and any electric energy supplied to the FP (e.g., for pumps, compressors, etc.) divided by η_{EE} – the efficiency of the power source (grid or the fuel cell). Normalizing the electric energy input with the efficiency helps evaluate the system on the basis of

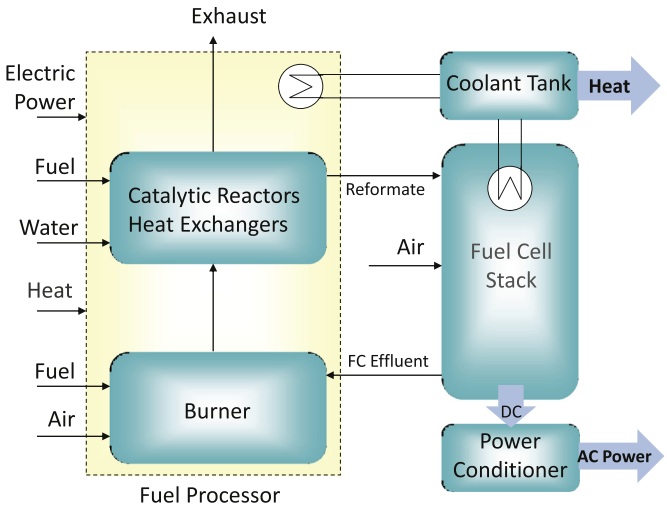

Fig. 1. Schematic of a generic CHP system.

the total thermal energy input into the system, since the output (numerator in Eq. (1)) is expressed in terms of the thermal energy equivalent. It is notable that the numerator and the second term in the denominator refer to only the hydrogen in the reformate stream because the low temperature fuel cell can only use hydrogen – other species, e.g., methane, nitrogen, etc., pass through as inerts or are present at trace levels. For higher temperature fuel cells where the hydrocarbon and carbon monoxide concentrations can be significant and can contribute to electrochemical power generation in the fuel cell, those terms should be defined to include these other species in the gas streams.

Eq. (2) defines the electrical efficiency of the fuel cell system as the net electric energy (DC power generated by the fuel cell minus any power redirected to operate pumps, blowers, heaters in the CHP system) as a percentage of the sum of LHV of the fuel supplied to the CHP system, any external heat inputs, and any electric power derived from the grid divided by the efficiency of the grid.

Eq. (3) defines the overall efficiency of the CHP system by including both the net electric energy and useful heat supplied externally in the numerator, divided by the energy inputs into the system as in Eq. (2). For the purposes of the simulations presented here, useful heat is defined as the heat transferred from the system coolant to a heat sink (residential hot water) and returning to the coolant tank at 60 °C.

3. System configuration C1

Fig. 2 shows an example system configuration (defined for this analysis) of a CHP system detailing more of the components and the flows within the fuel processor. The methane feed is injected into a stream of superheated steam and fed to a steam reformer (SR), with a H_2O/CH_4 or steam-to-carbon (S/C) ratio of 2–4. The steam reforming reaction, Eq. (4)

$$CH_4 + H_2O \rightarrow CO + CO_2 + H_2 \quad (4)$$

produces a reformate that leaves the SR at 600–800 °C and is quench-cooled to 325 °C by liquid water injection prior to entering the high temperature water gas shift reactor (HTS or WGS1), where the CO reacts with steam, Eq. (5)

$$CO + H_2O = CO_2 + H_2 \quad (5)$$

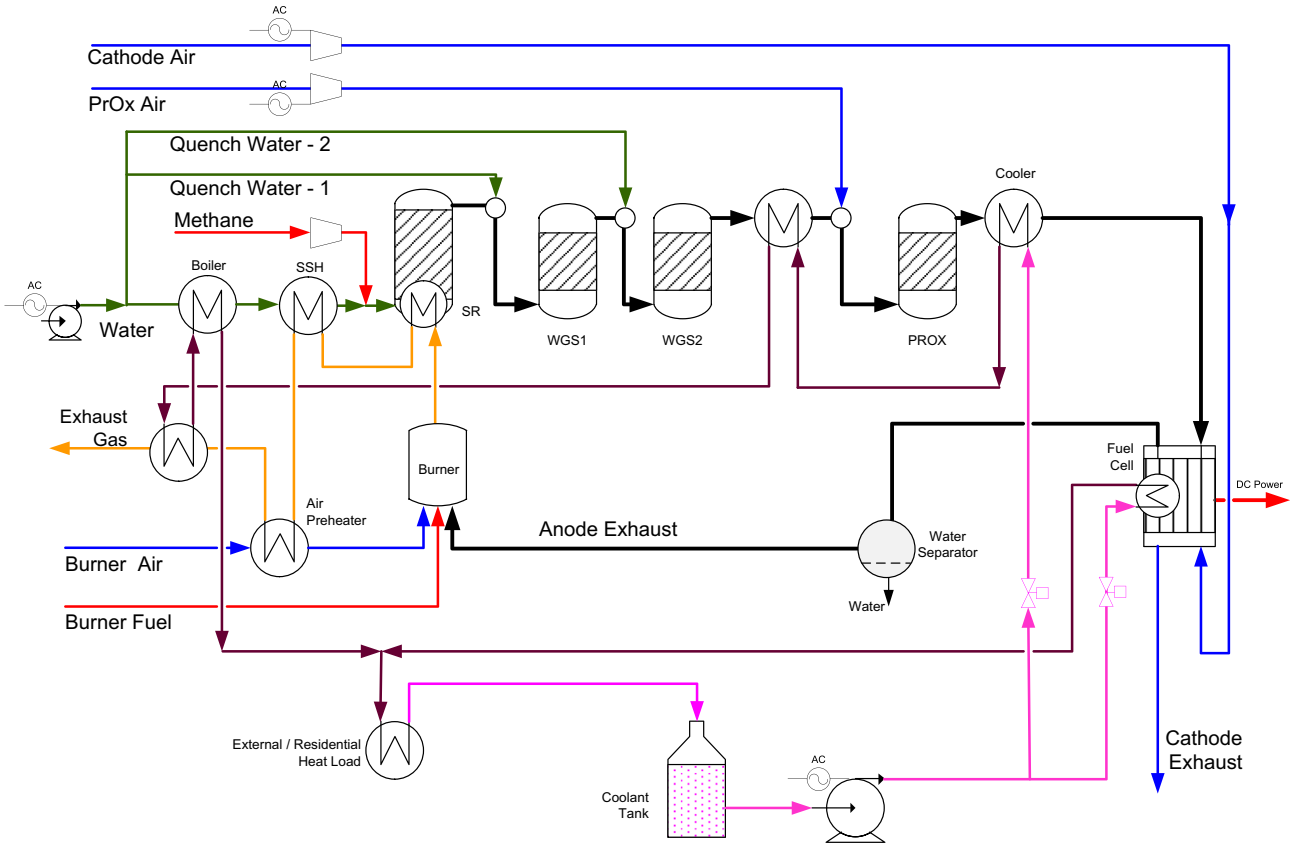

Fig. 2. System configuration C1: Quench cooling in the fuel processor.

The reformate is again quench cooled before entering the low temperature water gas shift reactor (LTS) at ~240 °C. The product gas from the second water-gas shift reactor is cooled by heat transfer to 115 °C prior to entering the preferential oxidation (PrOx) reactor designed to selectively oxidize the CO with oxygen from air,

3.1. Desired reaction

$$CO + 0.5O_2 = CO_2 \quad (6a)$$

3.2. Undesired reactions

$$H_2 + 0.5O_2 = H_2O \quad (6b)$$

$$CO + 3H_2 = CH_4 + H_2O \quad (6c)$$

The air to the PrOx reactor is specified at an $O_2/CO = 1$ molar ratio. The product reformate is cooled and then fed to the fuel cell anode. Since the reaction stoichiometry requires an $O_2/CO = 0.5$, the extra oxygen is assumed to react with the hydrogen in the reformate.

The hydrogen in the anode gas is electrochemically oxidized with the oxygen from air in the cathode to generate electric power. The fuel cell stack is maintained at its operating temperature with coolant flow. The spent cathode air is vented, after recovering its sensible heat, at >60 °C.

Supplementary fuel (methane) is fed to the burner if more energy is needed than what can be provided by burning just the anode effluent stream. The air feed rate for the burner is set for a specified excess (10–25%) over the stoichiometric amount needed. The hot combustion gas from the burner is used to provide the heat of reaction in the steam reformer, to superheat the steam feed to the reformer, to preheat the combustion air, and to transfer sensible heat to the coolant, before leaving the system as exhaust gas at >120 °C.

Temperature control of the various streams is managed with a network of heat exchangers and coolant streams. The coolant, water at elevated pressure (~5 atm) is pumped from a tank maintained at 60 °C and split into two streams. One stream is sent to the fuel cell stack to maintain its temperature at 80 °C. The other stream is sent to the fuel processor to successively cool the post-PrOx reformate, the post-LTS reformate, the exhaust gas, and then transfers part of the recovered heat to generate the steam for the reformer. Both of the returning coolant streams contain significant amounts of useful sensible heat; the two are merged and used to provide heat to the thermal load of the application, i.e., hot water or space heating for the residence, before returning to the coolant tank. The total heat recovered from the system (and delivered to the residence) is calculated as the difference in the enthalpy between the inlet and outlet of the residential heat exchanger, from which the coolant emerges at 60 °C (which is also the temperature in the coolant tank).

The system model was set up and analyzed using the commercial software package ASPEN Plus. Some of the assumptions used in the model are as follows:

- There is no heat loss from the various components of the system, even though many of them operate at elevated temperatures.
- The SR, HTS, and LTS effluents are at thermodynamic equilibrium, except that no additional CH_4 is formed or consumed in the water gas shift reactors or the preferential oxidation reactors.
- The oxygen selectivity for CO in the PrOx reactor is 50%, i.e., 50% of the oxygen in the PrOx air reacts with CO, and 50% reacts with H_2.
- The electrochemical efficiency of the stack specifies the percentage of the energy released from the hydrogen oxidation reaction that is converted to electric power. The electrochemical efficiency is treated as an input parameter with an assigned value in the simulations.

Table 1 lists the key input and output parameters from the simulation of the C1 configuration for a base case set of conditions, using 1 mol s^{-1} of methane as the feed to the SR. Even though the analysis is for 1–10 kWe CHP system, the basis of 1 mol s^{-1} has been selected because: 1 mol of methane is more absolute than 1 (or 10) kWe of electric power because the output value is the result of numerous other parameters of the process, and it is easier to interpret the product distribution results when the input rate is unity. For the major system components:

1. Steam Reformer: With the system at ambient pressure and the reformer at 750 °C operated with a S/C ratio of 2.3, the SR converts 98% of the methane in the feed to hydrogen and carbon oxides.
2. Shift Reactors: The quench cooling of the reformer output by injecting liquid water cools the WGS1 feed to 325 °C, and the WGS2 feed to 240 °C. Using this option to cool the shift reactor feed gases benefits the system by
   a. eliminating heat exchangers that add to the cost and thermal mass of the system, and
   b. increasing the H_2O/CO ratio which promotes CO conversion.
3. Fuel Cell Stack: With the fuel utilization of 77% listed in Table 1, the fuel cell stack electrochemically converts 77% of the hydrogen it receives from the FP. Operating at an electrochemical

Table 1
Input and output parameters from the simulation of the base case in C1.

Parameters	Unit	Input	Output
System pressure	psia (atm)	15 (1.02)	
Methane feed to SR (Basis)	mol s^{-1}	1	
Water to SR	mol s^{-1}	2.3	
SR exit temperature	°C	750	
CH_4 conversion in SR	%		98.2
Quench water − 1	mol s^{-1}		1.36
HTS inlet temperature	°C	325	
HTS outlet temperature	°C		417
Quench water − 2	mol s^{-1}		0.77
LTS inlet temperature	°C	240	
LTS outlet temperature	°C		261
H_2 in LTS product	mol s^{-1}		3.91
CH_4 in LTS product	mol s^{-1}		0.018
CO in LTS product	mol s^{-1}		0.020
CO_2 in LTS product	mol s^{-1}		0.962
O_2/CO molar ratio in PrOx feed		1	
Reformate from fuel processor to fuel cell			
H_2	mol s^{-1}		3.89
CO_2	mol s^{-1}		0.98
CH_4	mol s^{-1}		0.02
N_2	mol s^{-1}		0.076
Fuel (H_2) utilization	%	77	
Electrochemical efficiency	%	50	
Electric power (gross)	kWe		362
Heat recovered from FC by coolant	kW		362
Cathode air stoichiometry		2.5	
Blower power for cathode air	kWe		1.3
Supplemental CH_4 feed to burner	mol s^{-1}		0.20
Excess air to burner	%	25	
Exhaust gas temperature	°C		125
Fuel processor efficiency	%		79.7
Net electric power	kWe		361
Electrical efficiency	%		37.4
Total heat recovered by coolant	kW		375
CHP efficiency	%		76.4

efficiency of 50%, the stack generates 362 kWe of gross power and another 362 kW of heat that is removed by the coolant stream. On the cathode side, the air stoichiometry was specified at 2.5 (i.e., 150% excess air or 40% oxygen utilization) requiring 1.3 kWe of blower power. The high excess air has several advantages:

a. it maintains higher oxygen concentrations across the fuel cell active area, helping to promote the relatively slow oxygen reduction reaction in the cathode;
b. facilitates the removal of water produced in the cathode; and
c. can help to blow out any water droplets flooding the cathode flow channels.

4. Fuel Processor Burner: The anode effluent, containing the unreacted hydrogen and any unconverted methane are then burned in the FP burner, together with 0.2 mol s^{-1} of supplemental methane. The supplemental methane is needed to ensure that the SR can operate at 750 °C.

4. Results and discussion

For the base case system shown in Fig. 2 with the design and operating parameters listed in Table 1, the fuel processor efficiency (η_{FP}) was calculated to be 79.6%. The electrical and heat output from the system were 360 kWe of net electrical power and 375 kWt of heat delivered by the coolant to the residence, which values correspond to an electrical efficiency (η_{El}) of 37.4% and a combined heat and power efficiency (η_{CHP}) of 76.3%, respectively, based on the lower heating value of the natural gas fed to the CHP system.

The thermal energy recovered from the CHP system is primarily the waste heat from the fuel cell stack (362 kWt) available at a 80 °C, with the balance (~13 kWt) derived from the FP burner exhaust gas. The latter heat is of higher quality, available at over 120 °C. The parasitic power used by the pumps and blowers in the FP subsystem is small (<0.5 kWe) and this parasitic power does not affect the value of η_{FP}, even after normalizing with the system's electrical efficiency. The largest component of the parasitic power is the blower/compressor for the cathode air, which requires 1.3 kWe.

Converting the basis from 1 mol s^{-1} of methane to 5 kWe of electric power for a residential CHP unit (i.e., multiplying all outputs by 5/360) would generate 5.2 kW of heat, sufficient to heat ~200 L min^{-1} (~7 gal min^{-1}) of water from 25 °C to 55 °C.

In the single-variable analyses that follow, only the specified parameter was varied, with all other parameters maintained as in the base case (Table 1).

4.1. Effect of pressure

Increasing the system pressure affects the fuel processor by reducing the methane conversion in the reformer, reducing the hydrogen yield (also reported in previous experimental work with ethanol [23]). Increasing the pressure from the base case of 15 psia (1.02 atm) to 28 psia (1.9 atm) raises the unreacted methane almost 3-fold (from 0.018 to 0.53 mol s^{-1}), resulting in ~4% lower amount of hydrogen fed to the fuel cell (Table 2 and Fig. 3). The lower hydrogen to the fuel cell reduces the gross electrical power output, from 362 kWe at 15 psia to 349 kWe at 28 psia. However, the power required to compress the gas feeds, particularly the cathode air increases sharply with pressure, leading to almost 16% loss in net electric power.

As a result of the higher methane content in the reformate, which passes unreacted through the fuel cell, the anode effluent has a higher heating value. This lowers the amount of supplemental methane required in the burner, from 0.2 at 15 psia to 0.13 mol s^{-1} at 28 psia. The net effect of the lower methane conversion, hydrogen yield, and gross electric power output, and the higher parasitic power demand, is reflected in the efficiencies, plotted in Fig. 4, showing that with increasing pressure the FP efficiency increases, the electrical efficiency decreases, while the combined effect seen in the CHP efficiency passes through a minimum. Within the range studied, the electrical and CHP efficiencies are highest at the lowest pressure (15 psia).

Table 2
Effect of pressure on the CHP system.

System pressure	psia	15[a]	22	28
CH_4 in reformate to fuel cell	mol s^{-1}	0.018	0.036	0.053
H_2 in reformate to fuel cell	mol s^{-1}	3.89	8.82	3.75
Electric power (gross)	kWe	362	356	349
Compressor power	kWe	1.7	27.7	44.8
Net electric power	kWe	360.3	328.3	304.2
Supplemental CH_4 to burner	mol s^{-1}	0.20	0.17	0.13
FP efficiency	%	79.6	79.9	80.6
Electrical efficiency	%	37.4	35.0	33.6
CHP efficiency	%	76.3	74.6	75.3

[a] Base case.

There are other effects of pressure that could not be quantified in this study. For example, with higher pressures the components become heavier and more costly. The combination of high temperature and pressure in the reformer can become a significant challenge. Heavier components increase the thermal mass of the system, which can increase the amount of fuel required to reach operating temperatures during start-up. For systems requiring daily start-ups and shutdowns this fuel penalty can become significant over the lifecycle.

On the other hand, the higher reactant partial pressures favor the reaction kinetics which will lead to a volumetric shrinkage of the reactors and the fuel cell. Since the material cost (e.g., platinum) in the fuel cell is a significant contributor to the system's capital cost, a reduction in the total cell area (membrane electrode assembly) will lower the cost of the fuel cell and therefore, the system.

4.2. Effect of reformer temperature

Higher reformer temperatures (T_R) increase methane conversion in the reformer, increasing the total hydrogen yield from the fuel processor. The effects on hydrogen and methane feeds to the fuel cell are shown in Fig. 5. The plots show an 18% increase in H_2 and an 88% reduction in CH_4 in the reformate as a result of

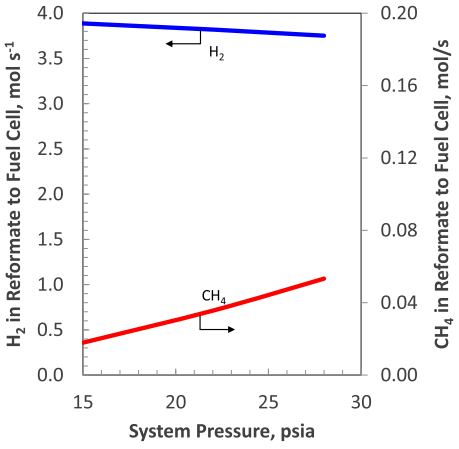

Fig. 3. Effect of pressure on hydrogen and methane in the reformate to the fuel cell. (SR Temperature = 750 °C, S/C to SR = 2.3, Fuel Utilization = 0.77).

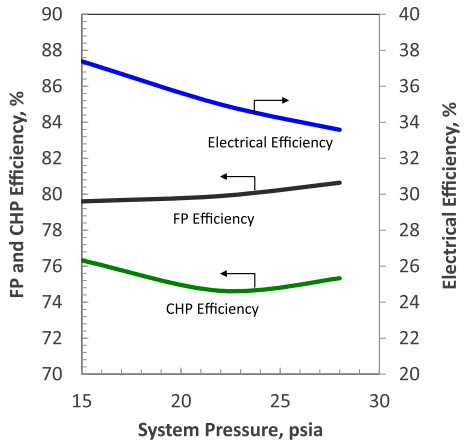

Fig. 4. Effect of pressure on efficiencies. (SR Temperature = 750 °C, S/C to SR = 2.3, Fuel Utilization = 0.77).

increasing the reformer temperature from 650° to 790 °C. The increased hydrogen yield increases the net electric power by almost 18% (Fig. 6).

One effect of the higher T_R is that more water is required to quench the hotter SR product, successively increasing the mass flow into the shift reactors. The total water (feed to SR [2.3 mol s^{-1}] + quench after SR + quench after HTS) added to the FP, as a result of the higher quench demand, increases from 3.3 at T_R = 650 °C to 4.7 at T_R = 790 °C. The additional quench water is beneficial in that it favors the CO conversion in the shift reactors. However, the additional moisture in the reformate increases the load on the heat exchangers downstream.

As seen in Fig. 5, the methane content in the reformate (and therefore in the anode effluent) decreases with increasing reformer temperature. The lower LHV of the anode effluent in combination with the need to maintain the reformer at a higher temperature requires more supplementary methane in the burner, as shown in Fig. 7. The total methane to the system increases from 1.03 to 1.24 mol s^{-1}, a 20% increase. The net effects of the higher hydrogen yield, more electric power, and higher methane usage on the efficiencies are seen in Fig. 8. The FP efficiency is 79.4% at 650 °C because the hydrogen yield from the reformer is low. The η_{FP} passes through a maximum of ~81% at 700 °C, then falls off at higher temperatures because the increase in H_2 yield is small relative to the increased demand for supplementary methane. For the same reason the electrical efficiency peaks at 700 °C, and the CHP

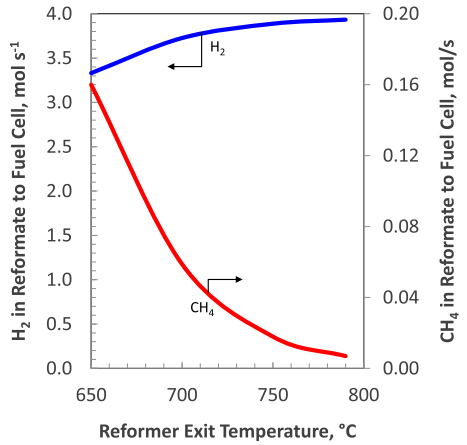

Fig. 5. Effect of reformer temperature on reformate to fuel cell. (P = 15 psia, S/C to SR = 2.3, Fuel Utilization = 0.77).

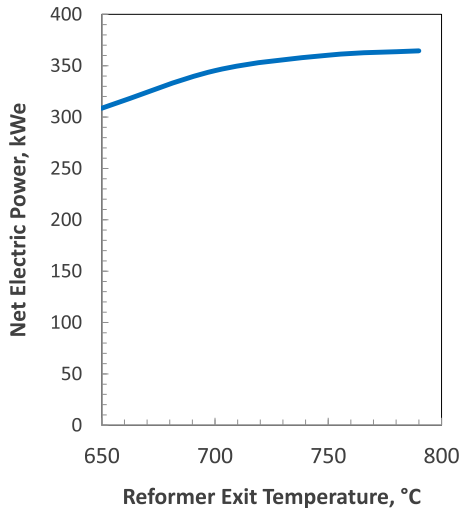

Fig. 6. Effect of reformer temperature on net electric power. (P = 15 psia, S/C to SR = 2.3, Fuel Utilization = 0.77).

efficiency curve shows a broader peak above 700 °C. Table 3 summarizes the effects on the key output parameters at the different simulated reformer temperatures.

Other qualitative considerations that factor into selecting the appropriate reformer temperature include:

- Higher temperatures may reduce the durability of the reforming catalyst.
- Higher reforming temperatures increases the needed temperature of the combustion gases to provide the heat of reaction, which can necessitate more refractory and expensive materials of construction, increasing the cost of the reformer.

4.3. Effect of steam-to-carbon ratio in the steam reformer

Steam reformers operate with excess steam to prevent coke formation (deposits of carbonaceous materials) and to promote higher conversion of the hydrocarbon. Higher levels of steam also shift the water–gas reaction equilibrium to the right, producing more hydrogen – the desired product for the fuel cell downstream. The higher methane conversion and higher hydrogen yield benefits

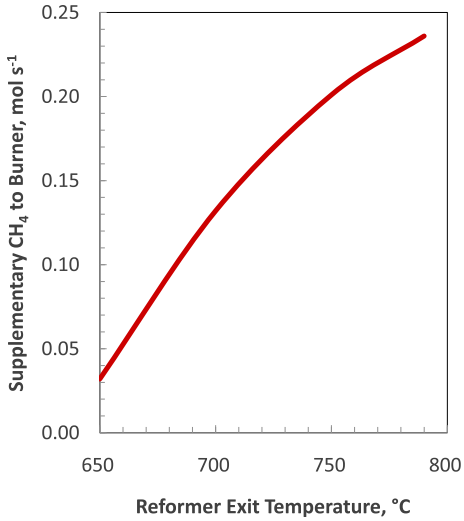

Fig. 7. Effect of reformer temperature on supplementary methane to burner. (P = 15 psia, S/C to SR = 2.3, Fuel Utilization = 0.77).

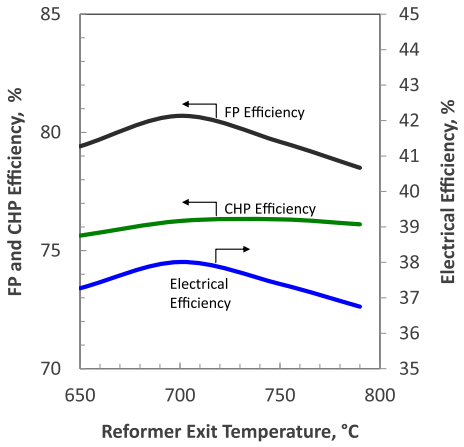

Fig. 8. Effect of reformer temperature on component and system efficiencies. (P = 15 psia, S/C to SR = 2.3, Fuel Utilization = 0.77).

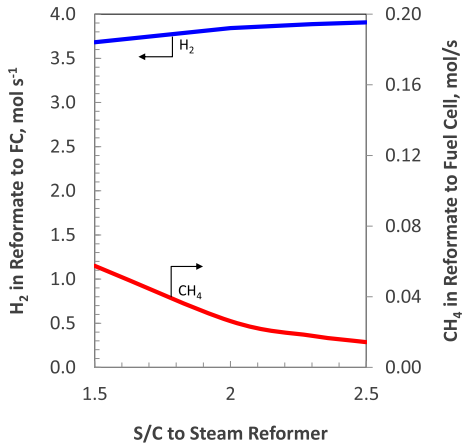

Fig. 9. Effect of steam-to-carbon ratio on the hydrogen and methane yield to the fuel cell. (P = 15 psia, SR Temperature = 750 °C, Fuel Utilization = 0.77).

the electric power output from the fuel cell. However, increasing the steam also has some drawbacks, which include: (i) generating the additional steam requires energy that is not usually recoverable cost-effectively, making for an inefficient process; (ii) maintaining the reformer temperature with the higher mass flow requires more energy from the burner; (iii) steam dilution reduces the concentration of other reactants, which may slow down the kinetics of other reactions downstream (e.g., in the PrOx or the fuel cell); (iv) the added mass flow enlarges the volume of reactor.

Fig. 9 shows the effect of the steam-to-carbon ratio in the SR on the flow rates of hydrogen and methane to the fuel cell, showing a 6% gain in H_2 and a 75% reduction in CH_4, as the S/C in the SR increases from 1.5 to 2.5. The corresponding net electric power output from the system increases from 341 to 362 kWe. The increase in S/C requires more water to quench the reformate, as shown in Fig. 10. Increasing the S/C from 1.5 to 2.5 in the SR, raises the total water feed to the FP from 3.30 to 4.71 mol s^{-1}, an increase of ~43%. The S/C increase, which increases methane conversion and lowers the LHV of the anode effluent, results in a ~16% increase in the supplementary methane requirement. The net effect on the efficiencies is shown in Fig. 11, showing a 4% improvement in the electrical efficiency, a 6% improvement in the FP efficiency, and an 8% reduction in the CHP efficiency resulting from the S/C increase across the range. The diminishing CHP efficiency reflects the fact that with increasing S/C more thermal energy is unrecoverable and is lost with the exhaust—the mass flow of the exhaust gas (leaving at 125 °C) is higher at the higher S/C conditions. The results are summarized in Table 4.

4.4. Effect of fuel (H_2) utilization in the fuel cell

Not all of the hydrogen entering the fuel cell anode is electrochemically oxidized. The reformate flow rate and the drawn current are balanced to maintain a desired cell voltage, which limits the hydrogen utilization of reformate based systems to well under 90%. While high fuel utilizations are desirable because the hydrogen has been produced by the fuel processor with some energy penalty (η_{FP} is indicative of the energy loss associated with the conversion of the primary fuel, CH_4, to H_2), the electrochemical performance of the cells diminishes at low hydrogen partial pressures. The design point fuel utilization is a trade-off between capital cost (of the fuel cell) and energy efficiency.

The gross electrical power output from the fuel cell is the product of the heating value of the hydrogen fed to the fuel cell, the fuel (hydrogen) utilization, and the electrochemical efficiency. Consequently, reducing the fuel utilization reduces the electrical output and leaves more hydrogen in the anode effluent. The anode effluent, which now has a higher LHV going into the FP burner, lowers the need for supplementary methane in the FP burner. When the LHV of the anode effluent exceeds the energy demand in the SR, the excess energy can either be recovered by the coolant stream or lost as sensible heat of the exhaust gas. Fig. 12 shows the effect of fuel utilization on the energy outputs from the system and the total methane feed into it. Lower fuel utilization reduces the electric power and the useful heat output from the fuel cell. An inflection point at ~60% fuel utilization represents the

Table 3
Effect of reformer temperature on the CHP system.

Reformer temperature, T_R	°C	650	700	750[a]	790
CH_4 in reformate to FC	mol s^{-1}	0.160	0.059	0.018	0.007
H_2 in reformate to FC	mol s^{-1}	3.33	3.73	3.89	3.93
Total quench water	mol s^{-1}	1.64	1.91	2.14	2.31
Net electric power	kWe	309	345	360	364
Supplementary CH_4 to burner	mol s^{-1}	0.03	0.13	0.20	0.24
FP efficiency	%	79.4	80.7	79.6	78.5
Electrical efficiency	%	37.3	38.0	37.4	36.8
CHP efficiency	%	75.6	76.3	76.3	76.1

[a] Base case.

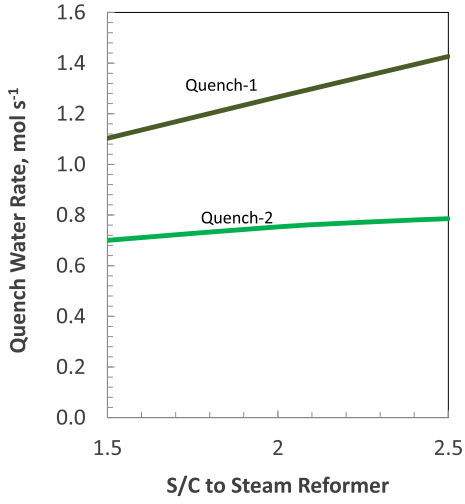

Fig. 10. Effect of steam to carbon (S/C) molar ratio on the water needed to quench the reformate. (P = 15 psia, SR Temperature = 750 °C, Fuel Utilization = 0.77).

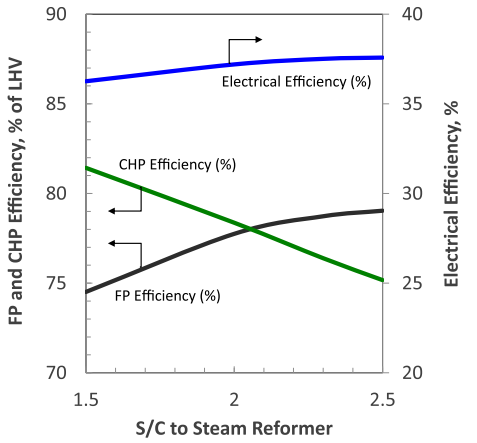

Fig. 11. Effect of steam-to-carbon ratio on the efficiencies. (P = 15 psia, SR Temperature = 750 °C, Fuel Utilization = 0.77).

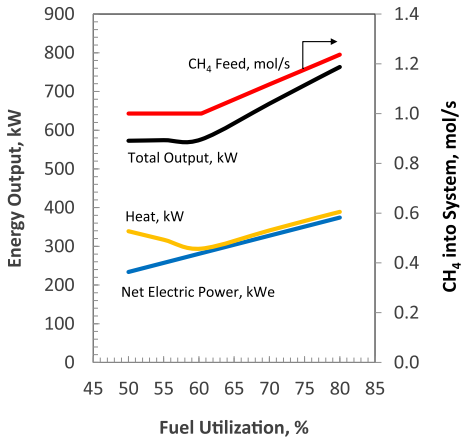

Fig. 12. Effect of fuel utilization on the fuel feed and energy outputs. (P = 15 psia, SRT = 750 °C, S/C = 2.3 (SR) + 1.36(QuenchWater-1) + 0.77(QuenchWater-2).

thermoneutral condition where the LHV of the anode effluent is sufficient to meet the heat demand in the steam reformer (i.e., requires no supplemental methane in the burner). At lower utilizations the total output remains flat, where the loss in electric output is balanced by the increase in the heat output. The effects on the efficiencies are shown in Fig. 13, with the electrical and FP efficiencies dropping off sharply at utilizations below the thermoneutral point, while the overall CHP efficiency flattens out. The results suggest that high fuel utilizations are preferred from efficiency considerations. This result supports the discussion above that since the hydrogen is produced at an efficiency of less than 100%, it should be advantageous to use the H_2 for electric power generation instead of generating heat in the burner. The results of the effect of fuel utilization are summarized in Table 5.

The results of the parametric study on the electrical and the total CHP efficiencies are summarized in Fig. 14, which shows that a combination of low pressure, high fuel utilization, low steam-to-carbon ratio and 700 °C reformer temperature offer opportunities for improving these two efficiencies. These results can be put in perspective by comparing them with some target values to see what changes may be needed for commercial deployment of such CHP systems.

5. Performance targets

In anticipation of commercial deployment of distributed CHP systems, the US Department of Energy has set some technical targets [24], some of which are shown in Table 6. The desired characteristics include the electrical and combined efficiencies of 42.5 and 87.5%, respectively. The combined efficiency target specifies that the heat should be available at 80 °C. For commercial success, the cost at high volume production should be limited to $8500 for a 5 kWe system ($1700 kWe^{-1}). For systems that may be turned off at night or for extended periods, the system should be able to reach its rated capacity within 30 min. These units should be robust, with a degradation rate of less than 0.5% per 1000 h of operation that includes cycling through start/stops and load following, and should last for 40,000 h with the end-of-life output that is no less than 80% of the original rated net power. Since the residential CHP unit is likely to go through start-up and shutdown cycles, and each cycle involves a start-up fuel penalty (energy consumed in heating the system to its operating temperature), the lifecycle efficiency – which also factors in the energy losses during start-ups and shutdowns, is also a useful measure.

The two columns at the far right in Table 6, indicate that with the system configuration C1, the highest electrical efficiency was calculated to be 38.1% at a steam reformer temperature of 700 °C, while maintaining all the other parameters at the base case conditions. This is more than 4 percentage points below the DOE target. Similarly, the highest CHP efficiency calculated in the parametric study was 81.4%, calculated at S/C = 1.5 and base case conditions. This value is more than 6 percentage points below the suggested

Table 4
Effect of the steam-to-carbon ratio to the SR on the CHP system.

Steam-to-carbon molar ratio to SR		1.5	2	2.3[a]	2.5
CH_4 in reformate to FC	mol s^{-1}	0.058	0.026	0.018	0.014
H_2 in reformate to FC	mol s^{-1}	3.68	3.84	3.89	3.91
Total quench water	mol s^{-1}	3.30	4.02	4.44	4.71
Net electric power	kWe	341	356	360	362
Supplementary CH_4 to burner	mol s^{-1}	0.177	0.197	0.201	0.205
FP efficiency	%	77.4	79.1	79.6	79.7
Electrical efficiency	%	36.1	37.1	37.4	37.5
CHP efficiency	%	81.4	78.3	76.3	75.1
Exhaust gas (125 °C) mass flow	mol s^{-1}	7.45	7.56	7.62	7.70

[a] Base case.

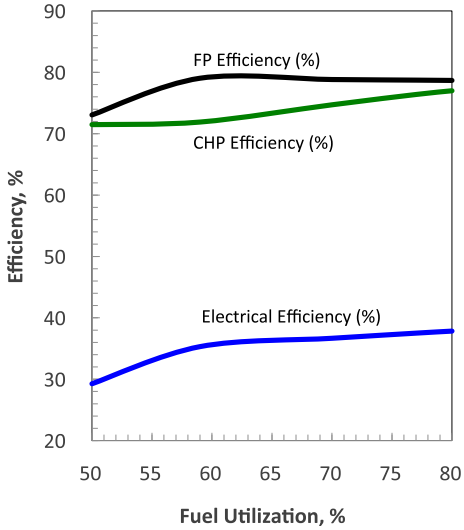

Fig. 13. Effect of fuel utilization on the efficiencies. (P = 15 psia, SRT = 750 °C, S/C = 2.3 (SR) + 1.36(QuenchWater-1) + 0.77(QuenchWater-2).

Table 5
Effect of fuel utilization on the CHP system.

Fuel utilization	%	55	60.4	70	77[a]	80
Net electric power	kWe	234	282	327	360	374
Supplementary CH_4 to burner	mol s^{-1}	0	0	0.117	0.201	0.237
Heat	kW	339	294	341	375	389
FP efficiency	%	73.8	79.9	79.7	79.6	79.56
Electrical efficiency	%	29.1	35.2	36.5	37.4	37.7
CHP efficiency	%	71.4	71.8	74.6	76.3	76.9

[a] Base case.

target, and the heat was available at 60 °C (the temperature of the coolant returning from the residential heat sink to the coolant tank in the CHP system).

5.1. Approaching performance targets with C1

Recognizing that the efficiency targets calculated thus far can be improved through a combination of parametric changes, the input specifications were revised for a high-performance C1 configuration to determine if they could meet the target efficiencies. The changed inputs are as follows (the other parameters were left unchanged):

- Steam-to-carbon molar ratio of 1.5;
- Steam reformer temperature of 700 °C;
- Fuel utilization of 80%;
- Electrochemical efficiency of 60%;
- Cathode air stoichiometry of 1.5. and
- Air stoichiometry at the FP burner of 1.1.

Table 7 shows some of the key inputs and outputs. By revising the parameters as indicated above, the electrical efficiency could be improved to 46%, which exceeds the target value of 42.5%. Although the revised parameters improved the CHP efficiency to 80.9%, it still fell short of the target value of 87.5%.

A true optimization of the C1 configuration would require inclusion of many other parameters that will balance the needs of cost, durability, start-up and transients, and other considerations discussed earlier.

5.2. Alternative system configuration C2

In an attempt to achieve higher performance levels, an alternative system configuration is shown in Fig. 15. In this

Table 6
Technical targets suggested for distributed CHP systems operating on natural gas in 2015 [24] compared to highest electrical and CHP efficiencies calculated from C1 simulations.

Performance, cost, durability	Unit	DOE target	η at T, S/C, …C1 (Fig. 14)	
Electrical efficiency, η_{El}	%	42.5	38.1	at $T_{SR} = 700$
CHP efficiency, η_{CHP}	%	87.5	81.4	at S/C = 1.5
Cost (50 K units/yr of 5 kWe systems)	\$ kWe^{-1}	1700		
Start-up time (from 20 °C)	min	30		
Operating lifetime (Time until >20% net power degradation)	h	40,000		
Degradation (with cycling)	%/1000-h	0.5		

configuration, the functions of the main process stream reactors remain the same, but instead of quench cooling of the reformate (before HTS and LTS), the temperature reduction is achieved by heat exchange cooling. The coolant from the heat exchanger between the PrOx and the LTS is now successively passed through the two new heat exchangers, before the recovered heat is used to generate the steam.

A second difference in this configuration is that water vapor is recovered from the anode effluent using a membrane separator to transfer it into the methane feed for the steam reformer. This water vapor recovery without the heat effects of phase change saves the energy that would otherwise be needed to generate the steam, thereby directly benefiting the system efficiency.

The performance results of a CHP system using the configuration C2 are shown in Table 8, where they are also compared to the values for the revised C1 scenario. Configuration C2 uses a higher steam-to-carbon ratio of 2.3 in the steam reformer, of which 0.3 is recovered in the vapor state from the anode effluent stream. The higher S/C (compared to 1.5 in the high performance version of configuration C1) increases the methane conversion and the hydrogen yield delivered to the fuel cell. However, since there is no water added to the reformate (as used in C1 for quenching), the H_2O/CO in the C2 shift reactors remain lower. Given the same exit temperatures from the shift reactors, the CO concentration of the LTS effluent is consequently higher in C2 (0.103) than in C1 (0.034).

More CO from the LTS requires more preferential oxidation reaction, which consumes hydrogen by the side reaction. The overall effect of higher methane conversion, higher hydrogen yield in the reformer, and more hydrogen consumption in the PrOx, is still

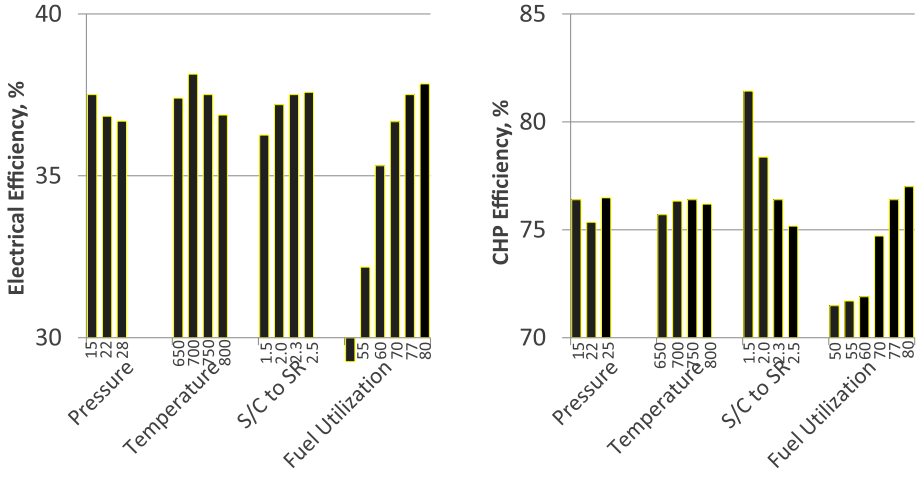

Fig. 14. Effect of operating conditions on efficiencies.

Table 7
Improved performance with revised parameters for C1.

Input parameters	Unit	C1 base case	C1 revised base case
S/C molar ratio		2.3	1.5
Steam reformer temperature	°C	750	700
Fuel utilization	%	77	80
Cathode stoichiometry		2.5	1.5
Electrochemical efficiency	%	50	60
Burner air stoichiometry		1.25	1.1
Output values			
H_2 in reformate to FC	mol s^{-1}	3.89	3.35
Supplementary CH_4 to burner	mol s^{-1}	0.20	0.051
Fuel processor efficiency	%	79.7	80.6
Net electric power	kWe	361	388
Electrical efficiency	%	37.4	46.0
CHP efficiency	%	76.4	80.9

Table 8
Comparison of the performance of the two configurations (all other input parameters are same).

Configuration	Unit	C1 (revised base case)	C2
S/C to steam reformer		1.5	2.3
Total water to FP	mol s^{-1}	3.09	2.3
CO in reformate from WGS to PrOx	mol s^{-1}	0.034	0.103
H_2 in reformate to FC	mol s^{-1}	3.35	3.56
Supplementary CH_4 to burner	mol s^{-1}	0.051	0.148
Fuel processor efficiency	%	80.6	78.8
Net electric power	kWe	388	408
Electrical efficiency	%	46.0	44.3
CHP efficiency	%	80.9	91.0

positive with the hydrogen yield in C2 (3.56 mol s^{-1}) being 6% higher than in C1 (revised). The greater amount of hydrogen fed to the fuel cell increases the electrical output – the net electrical power is 5% higher than in C1.

The lower methane content in the anode effluent and the higher mass flow in the steam reformer increases the supplementary methane required in the burner in C2. The net result is a lower fuel processor efficiency and a lower electrical efficiency. However, the additional heat recovered by the coolant contributes to the CHP efficiency, which is higher at 91%. Compared to the C1 configuration, C2 allows a trade-off between the electrical and CHP efficiencies. Compared to the high-performance (revised C1) system, the C2 system through its combination of added heat exchangers, higher S/C into the reformer, water vapor recovery from the anode effluent, has significantly improved the combined efficiency at an expense of a slightly lower electrical efficiency.

Introducing the two new heat exchangers in C2 has other implications that are not directly reflected in the metrics used in this analysis. The addition of the two heat exchangers and the membrane separator will increase the process complexity and add to the capital cost. Furthermore, the added thermal mass of the heat exchangers will increase the start-up fuel penalty (energy needed to heat the system up to operating temperatures), and will slow down the dynamic response to load changes.

Comparing with the DOE target where the heat is available at 80 °C, the heat recovery and CHP efficiency for this simulation was recalculated and was found to be 79.3% (instead of the 91% when based on a heat sink that is below 60 °C used in the simulation).

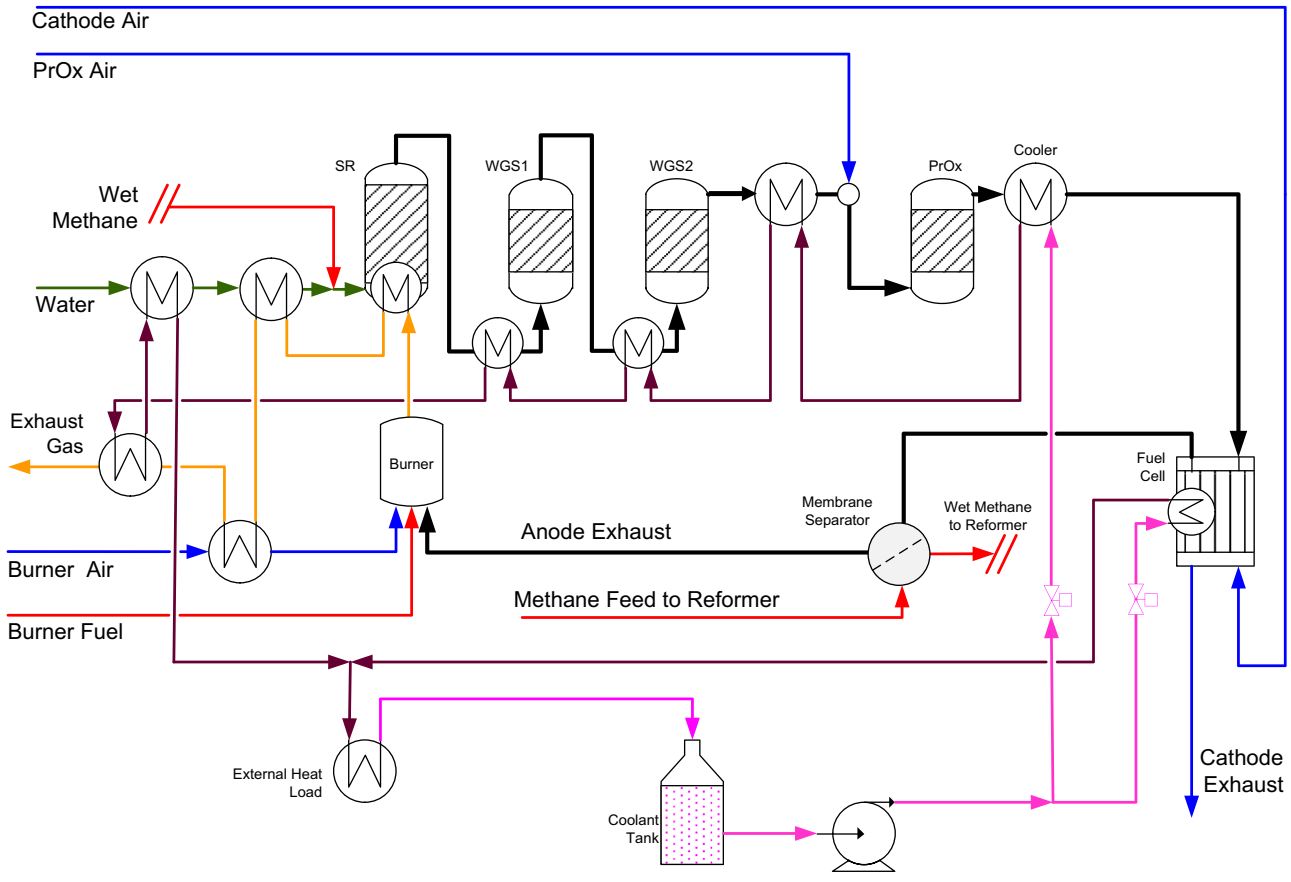

Fig. 15. Configuration C2 cools the reformate from the SR and the HTS in heat exchangers.

The above results are examples of the trade-offs that are possible by changing the design and operating parameters, and by changing the system configuration. These results show the potential of fuel cell-based CHP systems in recovering a high percentage of the fuel's heating value for use in residences. It should be noted that the values presented from the simulation are based on assumption of no heat loss, and for small systems the heat loss component can be significant, which makes attaining the DOE targets all the more difficult.

6. Summary and conclusions

A fuel cell-based combined heat and power system for residential applications has been analyzed to study the recovery of the fuel's heating value, and its distribution between heat and electricity. Two fuel processor configurations were evaluated – the first where temperature control was accomplished by using quench cooling. Analysis of the base case showed that the fuel processor efficiency, the electrical efficiency, and the CHP efficiency of 80%, 37%, and 76%, respectively, are possible. A study of the effect of select parameters in the first configuration (C1) showed that lower system pressures favor higher hydrogen yield and use less energy for compression, yielding higher net electrical output; raising the reformer temperature above 700 °C does not benefit the methane conversion sufficiently to offset the higher demand for supplementary methane; low S/C benefits the CHP efficiency but not the fuel processor and electrical efficiencies; and, the efficiencies are favored by high fuel utilizations. Applying these lessons can improve the performance of the CHP system, especially the electrical efficiency to 46%. Using configuration C2, which adds two heat exchangers and a membrane separator to recover water vapor from the anode effluent, allowed the overall CHP efficiency to 90%, with a small decrease in the electrical efficiency.

Acknowledgments

This work was supported by the U.S. Department of Energy's Fuel Cell Technologies Program Office. Argonne National Laboratory is managed for the U.S. Department of Energy by UChicago Argonne, LLC, under contract DE-AC-02-06CH11357.

References

[1] A.U. Dufour, J. Power Sources 71 (1998) 19–25.
[2] J.E. Brown, C.N. Hendry, P. Harborne, Energy Policy 35 (2007) 2173–2186.
[3] D.L. Greene, K. Duleep, G. Upreti, Status and Outlook for the U.S. Non-automotive Fuel Cell Industry: Impacts of Government Policies and Assesment of Future Opportunities, Oak Ridge National Laboratory - ORNL/TM-2011/101. Oak Ridge, Tennessee (2011).
[4] G. Upreti, D.L. Greene, K. Duleep, R. Sawhney, Int. J. Hydrogen Energy 37 (2012) 6339–6348.
[5] W.G. Colella, J. Power Sources 118 (2003) 129–149.
[6] Y. Isobe, Progress of the Japanese Commercial PEMFC System, Fuel Cell Seminar, Uncasville, CT, 2012.
[7] A. Scaramelli, Fuel Cells in Commercial Office Buildings. Why and How It Makes Sense, Fuel Cell Seminar, Uncasville, CT, 2012.
[8] H. Aki, Y. Taniguchi, I. Tamura, A. Kegasa, H. Hayakawa, Y. Ishikawa, S. Yamamoto, I. Sugimoto, Int. J. Hydrogen Energy 37 (2012) 1204–1213.
[9] N. Briguglio, M. Ferraro, G. Brunaccini, V. Antonucci, Int. J. Hydrogen Energy 36 (2011) 8023–8029.
[10] H.S. Chu, F. Tsau, Y.Y. Yan, K.L. Hsueh, F.L. Chen, J. Power Sources 176 (2008) 499–514.
[11] M. Ferraro, F. Sergi, G. Brunaccini, G. Dispenza, L. Andaloro, V. Antonucci, J. Power Sources 193 (2009) 342–348.
[12] C.E. Hubert, P. Achard, R. Metkemeijer, J. Power Sources 156 (2006) 64–70.
[13] G. Gigliucci, L. Petruzzi, E. Cerelli, A. Garzisi, A. La Mendola, J. Power Sources 131 (2004) 62–68.
[14] H. Adachi, S. Ahmed, S.H.D. Lee, D. Papadias, R.K. Ahluwalia, J.C. Bendert, S.A. Kanner, Y. Yamazaki, J. Power Sources 188 (2009) 244–255.
[15] E. Calo, A. Giannini, G. Monteleone, Int. J. Hydrogen Energy 35 (2010) 9828–9835.
[16] T. Fukunaga, H. Katsuno, H. Matsumoto, O. Takahashi, Y. Akai, Catal. Today 84 (2003) 197–200.
[17] J.G.D. Furtado, G.C. Gatti, E.T. Serra, S.C.A. de Almeida, Int. J. Hydrogen Energy 35 (2010) 9990–9995.
[18] F. Cipiti, V. Recupero, L. Pino, A. Vita, M. Lagana, J. Power Sources 157 (2006) 914–920.
[19] Independent Review Published for the U.S, Department of Energy Hydrogen and Fuel Cells Program, 1–10 kW Stationary Combined Heat and Power Systems Status and Technical Potential, National Renewable Energy Laboratory, NREL/BK-6A10-48265, 2012, 1–156.
[20] ENE FARM Residential Fuel Cells Launched: www.tokyo-gas.co.jp/tgminutes/64.pdf, [last accessed 01/03/13].
[21] ClearEdge5 system: www.clearedgepower.com, [last accessed 01/03/13].
[22] B.D. James, J. Perez, K.N. Baum, A. Spisak, M. Sanders, Low Temperature PEM Stationary Fuel Cell System Cost Analysis, Fuel Cell Seminar, Orlando, FL, 2011.
[23] D.D. Papadias, S.H.D. Lee, M. Ferrandon, S. Ahmed, Int. J. Hydrogen Energy 35 (2010) 2004–2017.
[24] U.S. Department of Energy, Energy Efficiency and Renewable Energy, "Hydrogen, Fuel Cells & Infrastructure Technologies Program Multi-year Research, Development and Demonstration Plan (2011).www.eere.energy.gov/hydrogenandfuelcells [last accessed 01/02/13].